

Warner-Lambert Pharmaceutical Co. (L.M.T.); National Science Foundation (Grant No. GP-34532) (R.J.M.).

Registry No. $[(\text{C}_6\text{H}_5)_3\text{PH}]_3\text{PrCl}_6$, 16949-62-5.

Supplementary Material Available: Listing of structure factor amplitudes (24 pages). Ordering information is given on any current masthead page.

References and Notes

- (1) As an illustration of the burgeoning of this field, a series of books (three already published) have come out since 1968 entitled "Halides of the Transition Elements", Wiley-Interscience, New York, N.Y.
- (2) A series of papers discuss these: L. B. Asprey et al., *Inorg. Chem.*, **3**, 126, 727 (1964); **5**, 659 (1966).
- (3) W. H. Zachariassen, *Acta Crystallogr.*, **1**, 285 (1948).
- (4) S. Z. Ali, Ph.D. Dissertation, University of New Orleans, 1972.
- (5) J. D. Corbett, D. L. Pollard, and J. E. Mee, *Inorg. Chem.*, **5**, 761 (1966).
- (6) J. L. Ryan and C. K. Jorgenson, *J. Phys. Chem.*, **70**, 2845 (1966).
- (7) The conventional reliability index $R = \sum |kF_o| - |F_c| / \sum |kF_o|$ and a weighted reliability index $R_w = \sum w|kF_o| - |F_c| / \sum |kF_o|^2$ with $1/w = 1/\sigma^2$ are cited in the paper. Scattering factors for Pr^{3+} , Cl^- , P, and C are taken from the paper by D. T. Cromer and J. T. Waber, *Acta Crystallogr.*, **18**, 104 (1965), while the scattering factor curve for hydrogen and the anomalous dispersion corrections for Pr^{3+} , Cl^- , and P are from "International Tables for X-Ray Crystallography", Vol. III, Kynoch Press, Birmingham, England, 1968. The programs used are part of the crystallographic package for the PDP-10 developed at the University of New Orleans by J. N. Brown, L. R. Towns, R. J. Majeste, and L. M. Trefonas (1966-1976). The package includes a modification of the LSLAT routine (K. N. Trueblood), a series of data reduction programs, a series of direct-methods programs (including FAZC and MULTAN II), Patterson and Patterson superposition programs, block diagonal least-squares and Fourier programs, and a package of figure-drawing programs (including ORTEP developed by C. K. Johnson).
- (8) M. Choca, J. R. Ferraro, and K. Nakamoto, *J. Inorg. Nucl. Chem.*, **37**, 1425 (1975).
- (9) L. R. Morss and J. Fuger, *Inorg. Chem.*, **8**, 1433 (1969).
- (10) L. R. Morss, M. Siegal, L. Stenger, and M. Edelstein, *Inorg. Chem.*, **9**, 1771 (1970).
- (11) R. W. Schwartz, *Mol. Phys.*, **30**, 1909 (1975).
- (12) R. W. Schwartz, *Mol. Phys.*, **31**, 1909 (1976).
- (13) D. A. Wensky and W. G. Moulton, *J. Chem. Phys.*, **53**, 3957 (1970).
- (14) W. A. Hargreaves, *Phys. Rev. B*, **6**, 3417 (1972).
- (15) A. Kiel and K. R. German, *Phys. Rev. B*, **8**, 2353 (1973).
- (16) J. L. Ryan, *Inorg. Chem.*, **8**, 2053 (1969).
- (17) M. D. Glick and L. J. Radonovich, Abstracts of Papers, American Crystallographic Association Summer Meeting, 1970, p 90.
- (18) L. E. Sutton, Ed., *Chem. Soc., Spec. Publ.*, No. 11 (1958).
- (19) J. J. Daly, *J. Chem. Soc.*, 3799 (1964).

Contribution from the Department of Chemistry,
The University of Calgary, Calgary, Alberta, Canada T2N 1N4

Synthesis, Vibrational and Tin-119 Mossbauer Spectra, and Crystal and Molecular Structure of Tris(dimethyltin(IV)) Bis(orthophosphate) Octahydrate

J. P. ASHMORE, T. CHIVERS,* K. A. KERR,* and J. H. G. VAN ROODE

Received September 10, 1976

AIC60679P

A single-crystal x-ray diffraction study has shown that Me_2SnCl_2 and Na_2HPO_4 react in aqueous solution to give $(\text{Me}_2\text{Sn})_3(\text{PO}_4)_2 \cdot 8\text{H}_2\text{O}$. The colorless needle-shaped crystals are orthorhombic and belong to space group $Pn2_1a$ with $a = 22.578$ (4), $b = 9.395$ (2), $c = 11.100$ (2) Å, and $Z = 4$. The structure was solved by standard Patterson and Fourier methods and refined to a final R value of 0.080. The structure of $(\text{Me}_2\text{Sn})_3(\text{PO}_4)_2 \cdot 8\text{H}_2\text{O}$ consists of infinite "ribbons" extending through the crystal in the b direction. One tin atom (inner) is in an almost regular octahedral environment with trans methyl groups [$\text{C-Sn-C} = 178.1$ (14)°], and the other two tin atoms (outer) are in highly distorted octahedral configurations [$\text{C-Sn-C} = 145.4$ (16), 151.1 (15)°] due to weak coordination to two water molecules. The other water molecules form a three-dimensional network of hydrogen bonds involving the phosphate oxygen atoms. The tin atoms are linked by PO_4 tetrahedra to give eight-membered rings in chair configurations. The different tin environments cannot be distinguished by ^{119}Sn Mossbauer spectroscopy ($\delta = 1.17$; $\Delta = 3.68$ mm s $^{-1}$ at 77 K) although the line widths ($\Gamma_1 = 1.37$; $\Gamma_2 = 1.32$ mm s $^{-1}$) are somewhat broadened. It is suggested that the formation of $(\text{Me}_2\text{Sn})_3(\text{PO}_4)_2 \cdot 8\text{H}_2\text{O}$ in aqueous solution results from the condensation reaction between 2 mol of H_2PO_4^- and the polynuclear species $[(\text{Me}_2\text{Sn})_3(\text{OH})_4]^{2+}$.

Introduction

The reaction of dimethyltin dichloride with Na_2HPO_4 in aqueous solution produces white crystals previously assumed to be $\text{Me}_2\text{SnHPO}_4$.¹ We were unable to unambiguously assign a structure to this compound on the basis of infrared and ^{119}Sn Mossbauer spectral data,² and we therefore undertook a single-crystal x-ray structure determination which revealed the compound to be $(\text{Me}_2\text{Sn})_3(\text{PO}_4)_2 \cdot 8\text{H}_2\text{O}$. In this paper we discuss the synthesis and vibrational and ^{119}Sn Mossbauer spectra of $(\text{Me}_2\text{Sn})_3(\text{PO}_4)_2 \cdot 8\text{H}_2\text{O}$ in the light of the determined crystal and molecular structure. A preliminary report of the x-ray structure determination has appeared.³

Previous reports of x-ray structural determinations of dimethyltin compounds have been limited to derivatives of monobasic acids e.g., Me_2SnF_2 ,⁴ $\text{Me}_2\text{Sn}(\text{SO}_3\text{F})_2$,⁵ $\text{Me}_2\text{Sn}(\text{CNS})_2$,⁶ $\text{Me}_2\text{Sn}(\text{CN})_2$,⁷ $\text{Me}_2\text{Sn}(\text{NO}_3)_2$,⁸ and Me_2SnCl_2 .⁹ In Me_2SnX_2 compounds there is a tendency for the tin atoms to become hexacoordinate either via intermolecular association ($\text{X} = \text{F}, \text{SO}_3\text{F}, \text{CNS}, \text{CN}, \text{Cl}$) or via intramolecular coordination ($\text{X} = \text{NO}_3$). The extent of intermolecular association,

as determined by the geometry of the C-Sn-C arrangement, varies considerably. For $\text{X} = \text{F}$ or SO_3F the association is strong leading to octahedral geometry about tin and trans methyl groups. For more weakly associated structures the observed geometry about tin can be viewed as either distorted tetrahedral or distorted octahedral ($\text{C-Sn-C} = \text{ca. } 149^\circ$, $\text{X} = \text{CNS}$,⁶ CN ;⁷ $\text{C-Sn-C} = \text{ca. } 123^\circ$, $\text{X} = \text{Cl}$)⁹.

Experimental Section

Instrumentation. The following instruments were used to obtain spectroscopic data: infrared spectra, Perkin-Elmer 337; far-infrared spectra, Digilab FTS 16; Mossbauer spectra, spectrometer described previously in ref 10. Raman spectra were obtained using a He/Ne laser operating at 6328 Å, using collinear excitation, and viewing with a Cary 81 spectrophotometer.

Synthesis. Equimolar quantities of dimethyltin dichloride and $\text{Na}_2\text{HPO}_4 \cdot 2\text{H}_2\text{O}$ in aqueous solutions (ca. 0.5 M) were mixed and allowed to stand at room temperature. Elongated, needle-shaped, colorless crystals were slowly deposited. These crystals were filtered off, washed with water, and dried in an Aberhalden pistol at 80 °C (0.1 mm); yield 52%; dec pt >350 °C. Anal. Calcd for $(\text{Me}_2\text{Sn})_3(\text{PO}_4)_2 \cdot 8\text{H}_2\text{O}$: C, 9.23; H, 4.31. Found: C, 9.82, 9.59; H,

Table I. Crystal Data and Agreement Factors for $(\text{Me}_2\text{Sn})_3(\text{PO}_4)_2 \cdot 8\text{H}_2\text{O}$

Fw 780.3	$V = 2354 \text{ \AA}^3$
$a = 22.578 (4) \text{ \AA}$	$d_{\text{meas}} = 2.31 \text{ g cm}^{-3}$
$b = 9.395 (2) \text{ \AA}$	$d_{\text{calcd}} = 2.20 \text{ g cm}^{-3}$
$c = 11.100 (2) \text{ \AA}$	$\mu(\text{Cu K}\alpha) = 279.6 \text{ cm}^{-1}$
Space group $Pnma$	$\lambda 1.5418 \text{ \AA}$
$Z = 4$	$F_{000} = 1512$
Unweighted R factor (all reflections)	0.1097
Unweighted R factor (obsd reflections)	0.0801
Weighted R factor (all reflections)	0.0697
Weighted R factor (obsd reflections)	0.0638
$(\Sigma w\Delta^2/(m-n))^{1/2}$	4.1674 ^a

^a Standard deviation of an observation of unit weights.

3.55, 3.19. (Calcd for $\text{Me}_2\text{SnHPO}_4$: C, 9.81; H, 2.88.) The high C and low H analyses may have been due to loss of water of crystallization. Reliable Sn and/or P analyses could not be reproduced for this compound.

Data Collection and Crystal Data. The crystal chosen for data collection, of dimensions ca. $0.1 \times 0.2 \times 0.1 \text{ mm}$, was mounted about its needle axis, b , and sealed in glue. Unit cell and space group data were obtained from oscillation, and zero- and first-layer Weissenberg photographs, using nickel-filtered $\text{Cu K}\alpha$ radiation. The use of Mo radiation led to decomposition. Weissenberg photographs of the $h0l$ and $h1l$ zones and precession photographs of the $0kl$, $1kl$, and $hk0$ zones showed systematic absences for $0kl$, $k+l = 2n+1$; hkl , $h = 2n+1$. This information is consistent with the orthorhombic space groups $Pnma$ and $Pn2_1a$. Although statistical tests suggested the centrosymmetric space group $Pnma$, the sample showed strong second harmonic generation¹¹ which is possible only if the true space group is the noncentrosymmetric $Pn2_1a$. The crystal data are listed in Table I. Intensity data were collected on a Picker four-circle diffractometer, equipped with a graphite monochromator and operated in the θ - 2θ scan mode with a scan rate of 2° min^{-1} and a scan range of $(2.1 + 0.285 \tan \theta)^\circ$. Background counts were recorded for 40 s at either end of the scan. The orientation matrix and cell dimensions were refined by a least-squares method, involving the parameters of 12 high-angle reflections. Both hkl and $\bar{h}\bar{k}l$ reflections were recorded to a maximum 2θ value of 110° . The three standard reflections which were monitored after every 90 reflections showed no systematic trends. The data were corrected for absorption, Lorentz, and polarization factors. In a preliminary communication,³ absorption corrections were made by Gaussian quadrature, but the data used in this paper have been corrected for absorption by an analytical method. Although there are differences in thermal parameters derived from the two data sets, the positional parameters do not differ significantly. Of the 1586 unique reflections only 604 were considered as observed reflections [$I > 3\sigma(I)$].

Structure Solution and Refinement. The positions of the tin atoms were obtained from a sharpened, three-dimensional Patterson map

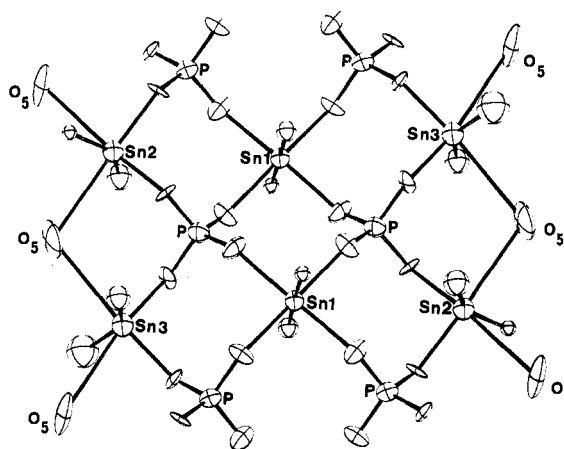


Figure 1. ORTEP drawing of $(\text{Me}_2\text{Sn})_3(\text{PO}_4)_2 \cdot 8\text{H}_2\text{O}$. Water molecules bonded to the two outer tin atoms are indicated as O_5 ; other water molecules are omitted for clarity.

and refined by the method of least squares. The phosphorus, phosphate oxygen, and carbon atoms were located from an electron density map, with phases calculated from the tin positions. Water molecules were located from a "difference Fourier" map. In the early stages of refinement by full-matrix least squares, one scale factor, extinction, and positional and isotropic temperature parameters were varied. In later stages a weighting scheme was introduced and anisotropic temperature factors were used for the tin, phosphorus, and oxygen atoms. The carbon atoms were refined isotropically. The hydrogen atoms were not located.

In order to resolve the ambiguity in the choice of space groups refinement was attempted in both $Pnma$ and $Pn2_1a$. No statistically significant improvement in the R value was obtained in going from $Pnma$ to $Pn2_1a$. This fact and the slow convergence in $Pn2_1a$ suggests that the positional and thermal parameters are best represented by the $Pnma$ data reported here. The deviation from $Pnma$ is discussed under "The Hydrogen-Bonding Scheme".

A compilation of observed and calculated structure factors is available as supplementary material. Agreement factors after the refinement had converged are shown in Table I. The final positional and thermal parameters are shown in Table II. The weighting scheme used was $w = (\sigma(F^2) + 0.0004F^2)^{-1}$. The scattering factors and anomalous scattering factors used were taken from literature sources.^{12,13}

Results and Discussion

Crystal Structure. The structure of $(\text{Me}_2\text{Sn})_3(\text{PO}_4)_2 \cdot 8\text{H}_2\text{O}$ consists of infinite ribbons extending through the cell in the b direction, as indicated in Figure 1. The dimethyltin groups are situated in special positions on the crystallographic mirror

Table II. Final Positional and Thermal Parameters for $(\text{Me}_2\text{Sn})_3(\text{PO}_4)_2 \cdot 8\text{H}_2\text{O}$ (Standard Deviations in Parentheses)

Atom	x	y	z	U_{11}^a	U_{22}	U_{33}	U_{12}	U_{13}	U_{23}
Sn(1)	0.5259 (1)	0.2500	0.4437 (3)	35 (2)	31 (2)	34 (2)	0	-6 (2)	0
Sn(2)	0.3390 (1)	0.2500	0.2431 (3)	40 (2)	36 (2)	43 (2)	0	-8 (2)	0
Sn(3)	0.6382 (1)	0.2500	0.8089 (3)	44 (2)	43 (2)	44 (2)	0	-7 (2)	0
P	0.4189 (4)	0.0009 (9)	0.3605 (8)	47 (7)	27 (6)	44 (6)	-3 (6)	-7 (5)	-1 (5)
O(1)	0.4748 (8)	0.0901 (22)	0.3492 (15)	41 (12)	49 (16)	43 (13)	-14 (13)	3 (12)	-12 (12)
O(2)	0.5838 (8)	0.0888 (20)	0.5213 (16)	53 (13)	36 (14)	49 (14)	10 (13)	-5 (12)	23 (12)
O(3)	0.3634 (7)	0.0948 (19)	0.3623 (14)	35 (11)	17 (13)	40 (13)	12 (11)	-5 (11)	16 (10)
O(4)	0.5820 (6)	0.0961 (18)	0.7534 (16)	26 (10)	31 (13)	44 (12)	-14 (10)	-7 (12)	-8 (12)
O(5)	0.6986 (9)	-0.0157 (31)	0.9068 (20)	42 (13)	127 (24)	98 (19)	-11 (16)	-41 (14)	-28 (20)
O(6)	0.3498 (9)	0.0905 (22)	0.8574 (17)	66 (15)	52 (16)	67 (16)	13 (14)	-6 (13)	-21 (13)
O(7)	0.3127 (9)	0.0799 (32)	0.6057 (19)	61 (16)	186 (33)	74 (18)	-40 (20)	32 (15)	-48 (19)
O(8)	0.4765 (9)	0.0694 (33)	0.8892 (18)	51 (15)	204 (36)	74 (17)	24 (21)	12 (14)	28 (21)
Atom	x	y	z	$\langle U^2 \rangle, \text{ \AA}^2 \times 10^3$	Atom	x	y	z	$\langle U^2 \rangle, \text{ \AA}^2 \times 10^3$
C(1)	0.5853 (15)	0.2500	0.2965 (30)	21 (10)	C(4)	0.4103 (19)	0.2500	0.1204 (36)	44 (13)
C(2)	0.4641 (16)	0.2500	0.5870 (34)	32 (12)	C(5)	0.6155 (20)	0.2500	0.9967 (46)	81 (19)
C(3)	0.2482 (16)	0.2500	0.2801 (32)	27 (11)	C(6)	0.7104 (17)	0.2500	0.6787 (36)	38 (13)

^a The values of U are multiplied by 10^3 . Anisotropic thermal parameters were used for Sn, P, and O atoms. The form of the anisotropic thermal ellipsoid is $\exp[-2\pi i^2(h^2 a^* U_{11} + k^2 b^* U_{22} + l^2 c^* U_{33} + 2hka^* b^* U_{12} + 2hla^* c^* U_{13} + 2klb^* c^* U_{23})]$.

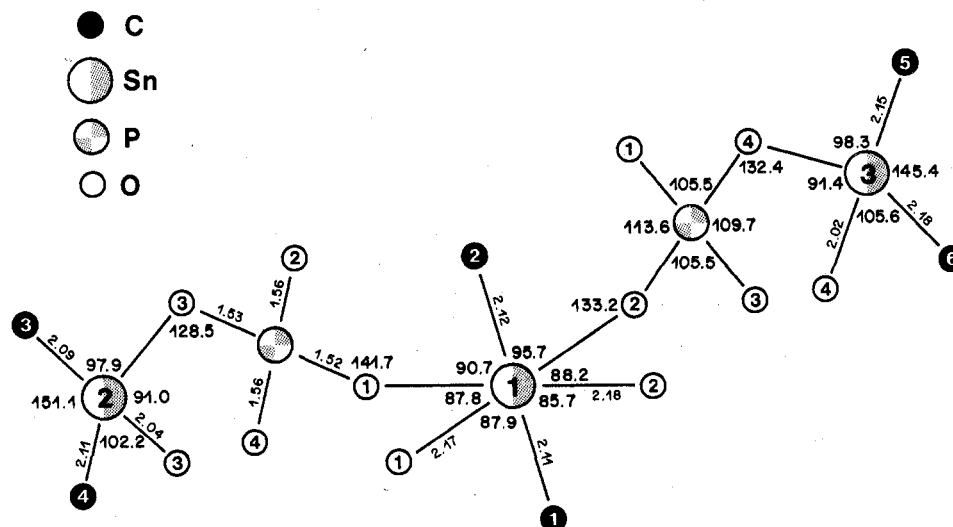


Figure 2. Principal bond distances and bond angles in $(\text{Me}_2\text{Sn})_3(\text{PO}_4)_2 \cdot 8\text{H}_2\text{O}$. Water molecules O(5) bonded to Sn(2) and Sn(3) are omitted.

Table III. Bond Distances (Å) in $(\text{Me}_2\text{Sn})_3(\text{PO}_4)_2 \cdot 8\text{H}_2\text{O}$

Sn(1)-O(1)	2.17 (2)	Sn(3)-O(4)	2.02 (2)
Sn(1)-O(2)	2.18 (2)	Sn(3)-O(5)	3.05 (3)
Sn(1)-C(1)	2.11 (3)	Sn(3)-C(5)	2.15 (5)
Sn(1)-C(2)	2.12 (4)	Sn(3)-C(6)	2.18 (4)
Sn(2)-O(3)	2.04 (2)	P-O(1)	1.52 (2)
Sn(2)-O(5)	2.89 (3)	P-O(2)	1.56 (2)
Sn(2)-C(3)	2.09 (4)	P-O(3)	1.53 (2)
Sn(2)-C(4)	2.11 (4)	P-O(4)	1.56 (2)

Table IV. Bond Angles (deg) in $(\text{Me}_2\text{Sn})_3(\text{PO}_4)_2 \cdot 8\text{H}_2\text{O}$

O(1)-Sn(1)-O(1)	87.8 (7)	O(4)-Sn(3)-C(5)	98.4 (10)
O(1)-Sn(1)-O(2)	91.6 (7)	O(4)-Sn(3)-C(6)	105.6 (8)
O(1)-Sn(1)-C(1)	87.9 (8)	O(5)-Sn(3)-O(5)	110.2 (7)
O(1)-Sn(1)-C(2)	90.7 (9)	O(5)-Sn(3)-C(5)	76.1 (8)
O(2)-Sn(1)-O(2)	88.2 (7)	O(5)-Sn(3)-C(6)	84.4 (7)
O(2)-Sn(1)-C(1)	85.7 (8)	C(5)-Sn(3)-C(6)	145.4 (16)
O(2)-Sn(1)-C(2)	95.6 (9)	O(1)-P-O(2)	113.5 (11)
C(1)-Sn(1)-C(2)	178.1 (14)	O(1)-P-O(3)	111.3 (11)
O(3)-Sn(2)-O(3)	91.0 (7)	O(1)-P-O(4)	105.5 (10)
O(3)-Sn(2)-O(5)	84.8 (7)	O(2)-P-O(3)	105.5 (10)
O(3)-Sn(2)-C(3)	97.9 (8)	O(2)-P-O(4)	111.5 (11)
O(3)-Sn(2)-C(4)	102.2 (9)	O(3)-P-O(4)	109.7 (10)
O(5)-Sn(2)-O(5)	99.4 (7)	Sn(1)-O(1)-P	141.7 (11)
O(5)-Sn(2)-C(3)	79.9 (7)	Sn(1)-O(2)-P	133.2 (11)
O(5)-Sn(2)-C(4)	81.5 (8)	Sn(2)-O(3)-P	128.5 (10)
C(3)-Sn(2)-C(4)	151.1 (15)	Sn(3)-O(4)-P	132.4 (10)
O(4)-Sn(3)-O(4)	91.4 (7)	Sn(2)-O(5)-Sn(3)	106.7 (7)
O(4)-Sn(3)-O(5)	78.7 (6)		

planes at $y = 1/4, 3/4$ and are linked by phosphate tetrahedra to give eight-membered rings in the chair configuration. A similar eight-membered ring system has been observed in the structure of the dimer $[(\text{SnCl}_3)_2(\text{PO}_2\text{Cl}_2)]_2$.⁸ A single water molecule and its symmetry equivalent occupy two coordination positions for each of the two outer tin atoms, Sn(2) and Sn(3). The other water molecules form a three-dimensional network of hydrogen bonds involving the phosphate oxygen. The principal dimensions of the structure are shown in Figure 2. Bond lengths and bond angles and nonbonded contacts are given in Tables III-VI. The three crystallographically independent tin atoms give rise to three different tin environments. The coordination about the inner tin atom Sn(1) is distorted only slightly from regular octahedral geometry, the octahedral angles ranging from 84 to 96°. The angle C(1)-Sn(1)-C(2) is 178.1 (14)°, close to a linear arrangement. The Sn(1)-C distances, 2.11 (5) and 2.12 (4) Å, are equal within experimental error and close to the single-bond value for octahedral tin,¹⁵ while the tin-oxygen bond lengths, Sn(1)-O(1) = 2.17 (2) Å and Sn(1)-O(2) = 2.18 (2)

Table V. Contact Distances (Å) between Nonbonded Oxygen Atoms in $(\text{Me}_2\text{Sn})_3(\text{PO}_4)_2 \cdot 8\text{H}_2\text{O}$

O(5)-O(3)	3.38 (3)	O(7)-O(2)	3.16 (3)
O(5)-O(4)	3.31 (3)	O(7)-O(3)	2.94 (3)
O(5)-O(6)	2.92 (3)	O(7)-O(7') ^a	3.20 (4)
O(5)-O(7)	2.73 (3)	O(8)-O(1)	3.23 (3)
O(6)-O(6') ^a	3.00 (3)	O(8)-O(4)	2.83 (3)
O(6)-O(7)	2.92 (3)	O(8)-O(8')	3.39 (4)
O(6)-O(8)	2.89 (3)	O(8)-O(8'') ^b	2.98 (3)

^a Symmetry-equivalent oxygen atoms related by a mirror plane.
^b Symmetry-equivalent oxygen atoms related by a center of inversion.

Table VI. Bond Angles (deg) with Nonbonded Oxygen Atoms as Apex in $(\text{Me}_2\text{Sn})_3(\text{PO}_4)_2 \cdot 8\text{H}_2\text{O}$

Sn(2)-O(5)-O(6)	102.9 (9)	O(3)-O(7)-O(6)	140.1 (9)
Sn(2)-O(5)-O(7)	119.9 (10)	O(3)-O(7)-O(7')	87.3 (9)
Sn(3)-O(5)-O(6)	110.5 (8)	O(5)-O(7)-O(6)	109.3 (9)
Sn(3)-O(5)-O(7)	97.7 (10)	O(5)-O(7)-O(7') ^a	109.2 (10)
O(6)-O(5)-O(7)	118.5 (10)	O(1)-O(8)-O(6)	105.6 (8)
O(5)-O(6)-O(6') ^a	103.9 (9)	O(1)-O(8)-O(8') ^a	117.6 (9)
O(5)-O(6)-O(7)	137.9 (10)	O(1)-O(8)-O(8'') ^b	110.6 (10)
O(5)-O(6)-O(8)	104.1 (8)	O(4)-O(8)-O(6)	139.7 (9)
O(2)-O(7)-O(5)	120.7 (11)	O(4)-O(8)-O(8')	84.9 (9)
O(2)-O(7)-O(6)	103.5 (8)	O(4)-O(8)-O(8'') ^b	100.3 (8)
O(2)-O(7)-O(7') ^a	120.1 (9)	O(6)-O(8)-O(8'') ^b	119.0 (9)
O(3)-O(7)-O(5)	109.6 (9)	O(8')-O(8)-O(8'') ^{a,b}	116.0 (10)

^a Symmetry-equivalent oxygen atoms related by a mirror plane.
^b Symmetry-equivalent oxygen atoms related by a center of inversion.

Å, are considerably longer than the single-bond value.¹⁵ The configuration about the outer tin atoms can be described as distorted octahedral with the water molecule O(5) and its symmetry equivalent occupying two positions in the coordination sphere of each tin atom (see Figure 1). Alternatively the outer tin environments can be viewed as highly distorted tetrahedral; the distortion toward octahedral was caused by weakly coordinated water molecules. Although the bond lengths involving the two outer tin atoms are similar, a comparison of bond angles shows marked differences in their geometrical environments. These are mainly due to the fact that coordination to water is different in the two cases. Thus the Sn-H₂O distances are 2.89 (3) and 3.05 (3) Å, respectively, for Sn(2) and Sn(3), and the H₂O-Sn-H₂O angles are significantly different [O(5)-Sn(2)-O(5) = 99.4 (7)°; O(5)-Sn(3)-O(5) = 110.2 (7)°]. The degree of distortion is best illustrated by the atoms that would be collinear in an undistorted octahedron. The C-Sn-C angles are 151.1 (15)

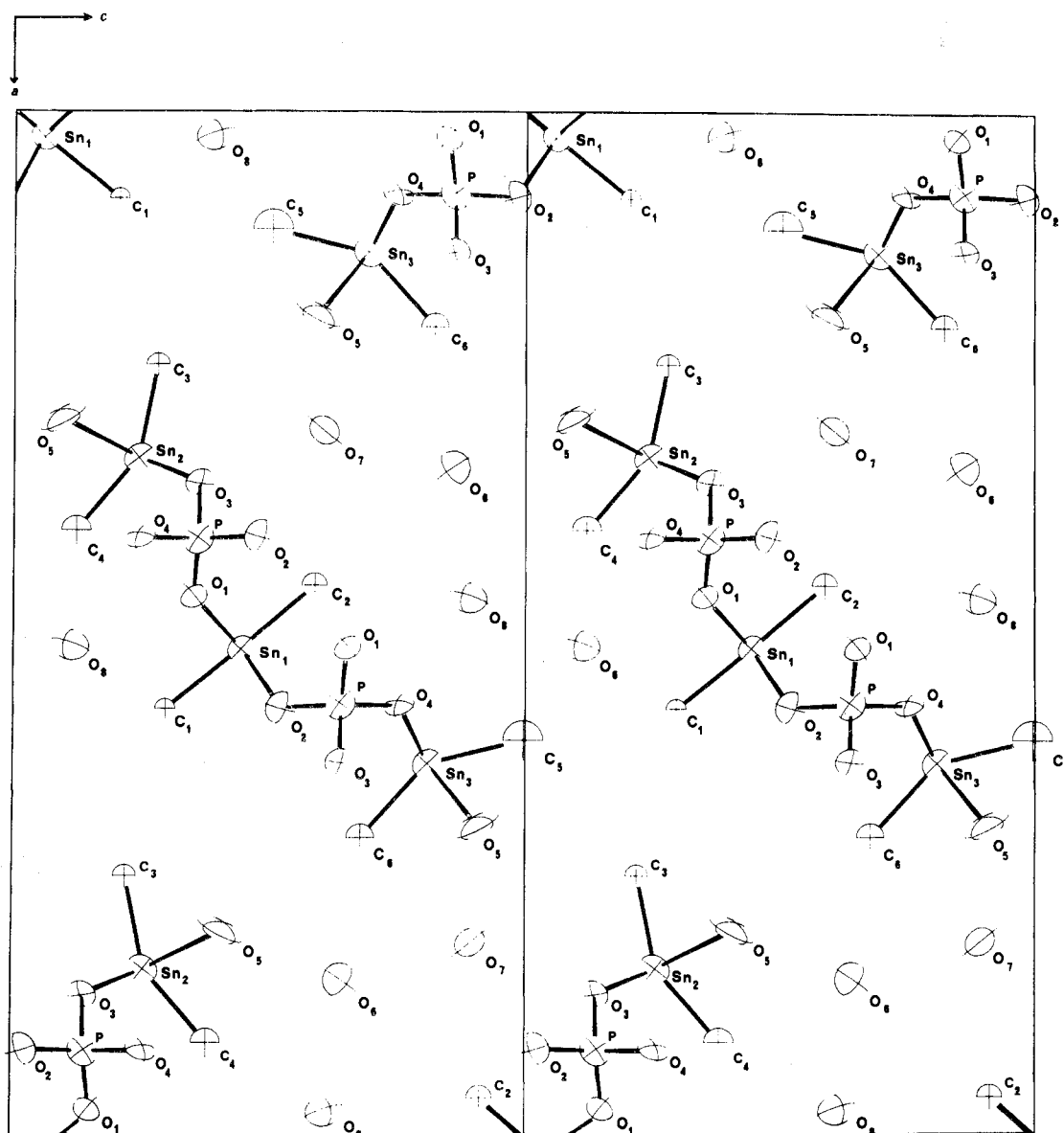


Figure 3. ORTEP drawing of $(\text{Me}_2\text{Sn})_3(\text{PO}_4)_2 \cdot 8\text{H}_2\text{O}$ viewed down the b axis with tin atoms at $y = 1/4$.

and $145.4 (16)^\circ$ for Sn(2) and Sn(3), respectively. The O(4)–Sn(3)–O(5) angle is $167.6 (7)^\circ$ while O(3)–Sn(2)–O(5) is $174.9 (7)^\circ$. Thus there are three distinct tin environments in the solid state of $(\text{Me}_2\text{Sn})_3(\text{PO}_4)_2 \cdot 8\text{H}_2\text{O}$. Figure 3 shows the $(\text{Me}_2\text{Sn})_3(\text{PO}_4)_2$ ribbons, viewed down the b axis, and the waters of crystallization that link them together. The ribbons have a fairly close approach to mm symmetry if one allows the second mirror plane to lie along the C(1)–C(2) axis. Apparently packing requirements for the space group $Pnma$ are the cause of the distortion from mm symmetry.

The Hydrogen-Bonding Scheme. The contact distances between the water oxygens and their nearest neighbors are shown in Figure 4. The O(5) water coordinates directly to the outer tins, Sn(2) and Sn(3). The phosphate oxygens are linked to O(6) by O(7) and O(8). O(6) coordinates only to water oxygens. The three oxygens O(6), O(7), and O(8) are approximately in the same y plane ($y \approx 0.8$). To arrive at a proposal for a hydrogen-bonding scheme the following considerations are important.

(a) In inorganic hydrates the principal features are that the hydrogen atoms of the water molecule are almost always involved in hydrogen bonds and that in the opposite direction, that of the negative end of the water dipole, there are almost

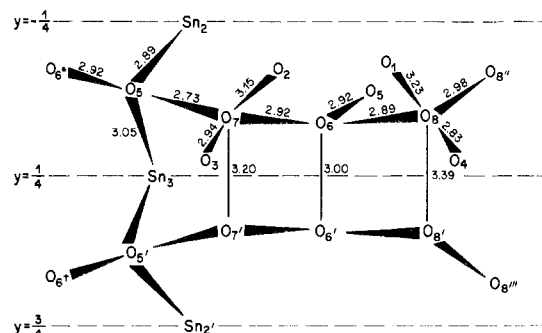


Figure 4. Contact distances between water oxygens and their nearest neighbors. Atom, symmetry-related position: O, x, y, z ; O', $x, 1/2 - y, z$; O'', $\bar{x}, \bar{y}, \bar{z}$; O*, $1/2 - x, \bar{y}, 1/2 + z$; O[†], $1/2 - x, 1/2 + y, 1/2 + z$; O''', $\bar{x}, 1/2 + y, \bar{z}$.

always one or more coordinated cations, or the water molecule is also acting as a hydrogen-bond acceptor.¹⁶

(b) Broadly speaking, a hydrogen bond is present when at least two heavy atom–hydrogen atom distances are less than the sum of the van der Waals radii present.¹⁶ The maximum O(donor)–O(acceptor) distance for which hydrogen bonding

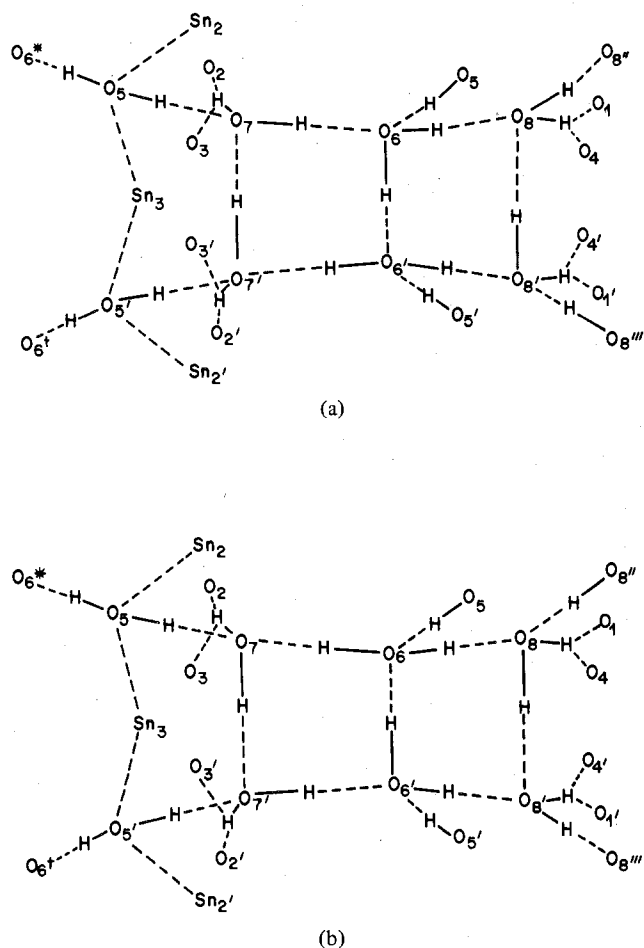


Figure 5. (a) Proposed hydrogen-bonding scheme for $(\text{Me}_2\text{Sn})_3(\text{PO}_4)_2 \cdot 8\text{H}_2\text{O}$. (b) Alternative hydrogen-bonding scheme for $(\text{Me}_2\text{Sn})_3(\text{PO}_4)_2 \cdot 8\text{H}_2\text{O}$.

is observed is $\sim 3.2 \text{ \AA}$;¹⁷ an O(donor)–O(acceptor) distance of $> 2.70 \text{ \AA}$ is considered to involve a “weak” hydrogen bond.

(c) The O(acceptor)–O(donor)–O(acceptor) angle varies from 80 to 130° .¹⁶

(d) The existence of bifurcated hydrogen bonds has been demonstrated in several inorganic hydrates, e.g., $\text{MgSO}_4 \cdot 4\text{H}_2\text{O}$.¹⁸

Figure 5 shows two possible hydrogen-bonding schemes which do justice to the above considerations. If both schemes were equally probable, then the actual structure would involve a statistical average of the two and $Pnma$ symmetry would be maintained on statistical grounds. Second harmonic generation has shown, however, that the structure is definitely noncentrosymmetric. This fact suggests that the alternative hydrogen-bonding schemes do not occur with equal probability and the true space group for the total structure, including hydrogen atoms, is therefore $Pn2_1a$. Both schemes show bifurcated hydrogen bonds from O(7) to the phosphate oxygens O(2) and O(3) and from O(8) to the phosphate oxygens O(1) and O(4). In the case of O(7), the contact distance O(7)–O(3) = $2.94(3) \text{ \AA}$ is somewhat shorter than the contact distance O(7)–O(2) = $3.15(3) \text{ \AA}$. However, O(2) and O(3) are sufficiently close together that a hydrogen bond from O(7) to one of them could also involve the other. In fact, the angles with O(7) as apex indicate that O(2) is a somewhat better choice in the tetrahedron around O(7) than O(3) (see Table VI). A similar situation occurs around O(8). The proposed hydrogen-bonding schemes involve the outer tin atoms Sn(2) and Sn(3), the phosphate oxygens, and the waters of crystallization.

Table VII. Solid-State Vibrational Spectrum (cm^{-1}) of $(\text{Me}_2\text{Sn})_3(\text{PO}_4)_2 \cdot 8\text{H}_2\text{O}$

Infrared ^a	Raman ^b	Assignment
3600–3100 s, b		$\nu(\text{OH})$
1625 w		$\delta(\text{H}_2\text{O})$
1170 m, sh		
1132 s		
1104 s		} $\nu_{\text{as}}(\text{PO}_4)$
1065 s		
1030 s		
888 s		
795 s		$\nu_s(\text{PO}_4)$
630 w, b		CH_3 rock
600 m, sh		$\delta_{\text{as}}(\text{PO}_4)$
590 m	589 mw	$\nu_{\text{as}}(\text{SnC}_2)$
	544 vs	$\nu_s(\text{SnC}_2)$
550 m		} $\delta_{\text{as}}(\text{PO}_4)$
520 m		
320		$\nu_{\text{as}}(\text{Sn-O})$
295		$\nu_s(\text{Sn-O})$
240		$\nu_{\text{as}}(\text{Sn-O})$

^a Key: s, strong; m, medium; w, weak; b, broad; sh, shoulder.

^b The Raman spectrum was only recorded in the Sn–C stretching region.

Synthesis of $(\text{Me}_2\text{Sn})_3(\text{PO}_4)_2 \cdot 8\text{H}_2\text{O}$. The formation of $(\text{Me}_2\text{Sn})_3(\text{PO}_4)_2 \cdot 8\text{H}_2\text{O}$ (rather than $\text{Me}_2\text{SnHPO}_4$) from dimethyltin dichloride and $\text{Na}_2\text{HPO}_4 \cdot 2\text{H}_2\text{O}$ in aqueous solution parallels the preparation of $\text{Sn}^{\text{II}}_3(\text{PO}_4)_2$ by addition of a 10% solution of Na_2HPO_4 to a saturated solution of acidified stannous sulfate.¹⁹ $(\text{Me}_2\text{Sn})_3(\text{PO}_4)_2 \cdot 8\text{H}_2\text{O}$, identified by its infrared and ^{119}Sn Mössbauer spectra (see below), was also obtained when aqueous solutions of dimethyltin dichloride and $\text{NaH}_2\text{PO}_4 \cdot \text{H}_2\text{O}$ were mixed. The behavior of the $\text{Me}_2\text{Sn}^{2+}$ cation in aqueous solution has been reviewed.²⁰ Below pH 2, the only species present is the aquodimethyltin(IV) ion $[\text{Me}_2\text{Sn}(\text{OH})_x]^{2+}$. Increasing the concentration leads to the formation of polynuclear species. Between pH 4 and 6 either $[(\text{Me}_2\text{Sn})_3(\text{OH})_4]^{2+}$ or $[(\text{Me}_2\text{Sn})_4(\text{OH})_6]^{2+}$ is formed; the optimal pH is 5.5.^{21,22} A further increase in the pH leads to breakdown of the polymeric species and at pH 8 the only soluble species is $\text{Me}_2\text{Sn}(\text{OH})_2$. The pH in the reaction mixture which led to the formation of $(\text{Me}_2\text{Sn})_3(\text{PO}_4)_2 \cdot 8\text{H}_2\text{O}$ was ca. 5, and at this pH $(\text{H}_2\text{PO}_4^-)/(\text{HPO}_4^{2-}) = 160$. Thus one can postulate that the initial reaction in the formation of $(\text{Me}_2\text{Sn})_3(\text{PO}_4)_2 \cdot 8\text{H}_2\text{O}$ is between 1 mol of $[(\text{Me}_2\text{Sn})_3(\text{OH})_4]^{2+}$ and 2 mol of H_2PO_4^- . Elimination of four molecules of water would lead to a product in which three dimethyltin groups are bridged by two phosphate groups. Clearly both pH and concentration are important factors in determining the products of the reactions of dimethyltin dichloride with phosphorus oxy anions in aqueous solution, but we have not studied the effect of these variables in detail.

Vibrational Spectra. Infrared and Raman data for $(\text{Me}_2\text{Sn})_3(\text{PO}_4)_2 \cdot 8\text{H}_2\text{O}$ are given in Table VII. A strong, broad band is observed in the infrared spectrum between 3600 and 3100 cm^{-1} , indicative of the presence of water of crystallization. The crystal structure of $(\text{Me}_2\text{Sn})_3(\text{PO}_4)_2 \cdot 8\text{H}_2\text{O}$ indicates the absence of any site symmetry for the phosphate groups. The infrared spectrum is consistent with this fact since $\nu_{\text{as}}(\text{PO}_4)$ is split into four strong bands in the 1000 – 1200-cm^{-1} region. $\delta_{\text{as}}(\text{PO}_4)$ is also split into at least three bands in the 400 – 600-cm^{-1} region. The strong band at 888 cm^{-1} is attributed to $\nu_s(\text{PO}_4)$, which is usually observed in the 950 – 1020-cm^{-1} region.²³ The low frequency indicates charge withdrawal from the P–O into the Sn–O bonds, consistent with covalent Sn–O bands. The Sn–C stretching region is obscured by the PO_4 bending vibrations. For the central tin atom, Sn(1), the C–Sn–C arrangement is almost linear and one expects to observe only $\nu_{\text{as}}(\text{SnC}_2)$ in the infrared spectrum and only $\nu_s(\text{SnC}_2)$ in the Raman spectrum. For the bent C–Sn–C

Table VIII. ^{119}Sn Mossbauer Quadrupole Splittings and C-Sn-C Angles for Me_2SnX_2

Compd	Δ , ^a mm s ⁻¹	C-Sn-C, deg	Ref
Me_2SnF_2	4.52	~180 (x ray)	4, 26
$\text{Me}_2\text{Sn}(\text{SO}_3\text{F})_2$	5.54	~180 (x ray)	5, 27
Me_2SnSO_4	5.00	~180 (IR)	27, 28
$\text{Me}_2\text{Sn}(\text{PO}_2\text{F}_2)_2$	5.13	~180 (IR/Raman)	29
$\text{Me}_2\text{Sn}(\text{PO}_2\text{H}_2)_2$	4.34, 4.36	~180 (IR/Raman) ^c	2, 29
$\text{Me}_2\text{Sn}(\text{NCS})_2$	3.87 ^b	~146 (x ray)	6, 30
$\text{Me}_2\text{Sn}(\text{NO}_3)_2$	4.13, 4.20	~145 (x ray)	8, 24, 31
Me_2SnCl_2	3.55	~123 (x ray)	9, 25
$(\text{Me}_2\text{Sn})_3(\text{PO}_4)_2 \cdot 8\text{H}_2\text{O}$	3.68	~180 ~150 (x ray) ~145	This work

^a At liquid nitrogen temperature. ^b At room temperature.

^c For $\text{Me}_2\text{Sn}(\text{PO}_2\text{H}_2)_2$, $\nu_s(\text{SnC}_2)$ is observed as a strong band at 517 cm^{-1} in the Raman spectrum but is absent in the infrared spectrum.

arrangements of the two outer tin atoms, Sn(2) and Sn(3), $\nu_s(\text{SnC}_2)$ and $\nu_{as}(\text{SnC}_2)$ should both be infrared and Raman active. In fact, $\nu_s(\text{SnC}_2)$ is observed as a very strong band at 544 cm^{-1} in the Raman spectrum but is hidden by the PO_4 bending vibrations in the infrared spectrum. $\nu_{as}(\text{SnC}_2)$ appears at 590 cm^{-1} in the infrared spectrum and at 589 cm^{-1} in the Raman spectrum. Apparently the frequency of this vibration is not significantly different for the two different C-Sn-C arrangements in $(\text{Me}_2\text{Sn})_3(\text{PO}_4)_2 \cdot 8\text{H}_2\text{O}$. In the far-infrared spectrum of $(\text{Me}_2\text{Sn})_3(\text{PO}_4)_2 \cdot 8\text{H}_2\text{O}$ three bands are observed in the $200\text{--}350\text{-cm}^{-1}$ region, at 240, 295, and 320 cm^{-1} . These bands are assigned to Sn-O stretching vibrations which, for methyltin nitrates,²⁴ are sensitive to Sn-O bond distances, the shorter Sn-O bonds being associated with the higher Sn-O stretching frequency. The 240-cm^{-1} band is therefore tentatively assigned to the longer Sn-O bonds of the central Sn(1) atom, and the bands at 320 and 295 cm^{-1} are assigned to $\nu_{as}(\text{SnO}_2)$ and $\nu_s(\text{SnO}_2)$, respectively, of the shorter Sn-O bonds in the distorted octahedral outer Sn(2) and Sn(3) environments.

^{119}Sn Mossbauer Spectra. ^{119}Sn Mossbauer data for the compound previously assigned the formula $\text{Me}_2\text{SnPO}_4\text{H}$ and now shown to be $(\text{Me}_2\text{Sn})_3(\text{PO}_4)_2 \cdot 8\text{H}_2\text{O}$ have been reported ($\delta = 1.19\text{ mm s}^{-1}$; $\Delta = 3.62\text{ mm s}^{-1}$).² (All δ and Δ values are $\pm 0.05\text{ mm s}^{-1}$; δ values are relative to BaSnO_3 .) The value of the quadrupole splitting is consistent with hexa- (or penta-) coordinate tin, but the line widths ($\Gamma_1 = 1.17\text{ mm s}^{-1}$, $\Gamma_2 = 1.15\text{ mm s}^{-1}$) now gave indication of more than one tin environment for this compound. We therefore remeasured the Mossbauer spectrum of $(\text{Me}_2\text{Sn})_3(\text{PO}_4)_2 \cdot 8\text{H}_2\text{O}$ after the crystal structure determination with essentially similar results, $\delta = 1.23\text{ mm s}^{-1}$ and $\Delta = 3.68\text{ mm s}^{-1}$ at 77 K and $\delta = 1.17\text{ mm s}^{-1}$ and $\Delta = 3.66\text{ mm s}^{-1}$ at 298 K, except that the line widths were somewhat broader ($\Gamma_1 = 1.37$, $\Gamma_2 = 1.32\text{ mm s}^{-1}$ at 77 K; $\Gamma_1 = 1.25$, $\Gamma_2 = 1.30\text{ mm s}^{-1}$ at 298 K) for the remeasured data.

Table VIII lists values of Δ for a number of Me_2SnX_2 compounds (X = inorganic anion) of known geometry in which the C-Sn-C angle varies from 123 to 180° depending on the degree of intermolecular association in the solid state. The data in that table shows that even for Me_2SnCl_2 with a tin environment that is severely distorted from trans-octahedral geometry, values of Δ are observed that are normally associated with a coordination number around tin of more than 4.²⁵ The dominant contribution to the z component of the electric field gradient (V_{zz}) comes from the methyl ligands. A decrease in the C-Sn-C angle from 180 to 150° reduces the contribution of the methyl ligands to V_{zz} by ca. 10%. The conclusion must be that the Δ (and δ) values for the outer tin atoms (with their distorted octahedral environment) are not

very different from the corresponding values for the central tin atom with its nearly regular octahedral environment, and therefore the different tin environments cannot be distinguished by Mossbauer spectroscopy.

Conclusion

This investigation is a convincing demonstration of the dubious value of Mossbauer spectroscopy for making conclusions about the similarity (or difference) in tin environments for organotin(IV) compounds containing more than one tin atom per formula unit, without the results of a single-crystal x-ray structure determination. The structure adopted by $(\text{Me}_2\text{Sn})_3(\text{PO}_4)_2 \cdot 8\text{H}_2\text{O}$ shows the same general feature as other dimethyltin(IV) compounds, i.e., a preference for hexacoordinate tin environments. The formation of $(\text{Me}_2\text{Sn})_3(\text{PO}_4)_2 \cdot 8\text{H}_2\text{O}$ from the reaction of dimethyltin chloride and Na_2HPO_4 in aqueous solution indicates that the products of the reactions of organotin halides and phosphorus oxy anions in aqueous solution will be dependent on such variables as pH and concentration.

Acknowledgment. The authors are grateful to Professor J. R. Sams and Dr. J. N. Ruddick for the redetermination of the Mossbauer spectrum of $(\text{Me}_2\text{Sn})_3(\text{PO}_4)_2 \cdot 8\text{H}_2\text{O}$ and to the National Research Council of Canada for financial support in the form of operating grants (T. C., K. A. K.), a post-graduate scholarship (J.H.G.V.R.), and a capital equipment grant for the purchase of the far-infrared spectrometer. Dr. J. P. Dougherty (Philips Laboratories, Briarcliff Manor, N.Y.) kindly performed the second harmonic generation test for centrosymmetry.

Registry No. $(\text{Me}_2\text{Sn})_3(\text{PO}_4)_2 \cdot 8\text{H}_2\text{O}$, 60909-13-9; dimethyltin dichloride, 753-73-1; $\text{Na}_2\text{HPO}_4 \cdot 2\text{H}_2\text{O}$, 10028-24-7; ^{119}Sn , 14314-35-3.

Supplementary Material Available: Listing of structure factor amplitudes (8 pages). Ordering information is given on any current masthead page.

References and Notes

- D. Seyferth and F. G. A. Stone, *J. Am. Chem. Soc.*, **79**, 515 (1957).
- T. Chivers, J. H. G. Van Roode, J. N. Ruddick, and J. R. Sams, *Can. J. Chem.*, **51**, 3702 (1973).
- J. P. Ashmore, T. Chivers, K. A. Kerr, and J. H. G. Van Roode, *J. Chem. Soc., Chem. Commun.*, 653 (1974).
- E. O. Schlemper and W. C. Hamilton, *Inorg. Chem.*, **5**, 995 (1966).
- F. H. Allen, J. A. Lerbscher, and J. Trotter, *J. Chem. Soc.*, 2507 (1971).
- R. A. Forder and G. M. Sheldrick, *J. Organomet. Chem.*, **22**, 611 (1970); Y. M. Chow, *Inorg. Chem.*, **8**, 794 (1970).
- J. Konnerd, D. Britton, and Y. M. Chow, *Acta Crystallogr., Sect. B*, **28**, 180 (1972).
- J. Hilton, E. K. Nunn, and S. C. Wallwork, *J. Chem. Soc., Dalton Trans.*, 173 (1973).
- A. G. Davies, H. J. Milledge, D. C. Puxley, and P. J. Smith, *J. Chem. Soc. A*, 2862 (1970).
- P. A. Yeats, B. L. Poh, B. F. E. Ford, J. R. Sams, and F. Aubke, *J. Chem. Soc. A*, 2188 (1970).
- J. P. Dougherty and S. K. Kurtz, *J. Appl. Crystallogr.*, **9**, 145 (1976).
- D. T. Cromer and J. B. Mann, *Acta Crystallogr., Sect. A*, **24**, 321 (1968).
- D. T. Cromer and D. Liberman, *J. Chem. Phys.*, **53**, 1891 (1970).
- D. Moras, A. Mitschler, and R. Weiss, *Acta Crystallogr., Sect. B*, **25**, 1720 (1969).
- L. Pauling, "The Nature of the Chemical Bond", 3d ed, Cornell University Press, Ithaca, N.Y., 1960, pp 229, 251.
- W. C. Hamilton and J. A. Ibers, "Hydrogen Bonding in Solids", W. A. Benjamin, New York, N.Y., 1968.
- G. Ferraris and M. Franchini-Angela, *Acta Crystallogr., Sect. B*, **28**, 3572 (1972).
- W. Baur, *Acta Crystallogr.*, **17**, 683 (1960).
- E. Jablczynsky and W. Wieckowsky, *Z. Anorg. Allg. Chem.*, **152**, 207 (1926).
- R. S. Tobias, *Organomet. Chem. Rev.*, **1**, 93 (1966).
- R. S. Tobias and M. Yasuda, *Can. J. Chem.*, **42**, 781 (1964).
- R. S. Tobias, I. Ogrins, and B. A. Bennett, *Inorg. Chem.*, **1**, 638 (1962).
- A. Hezel and S. D. Ross, *Spectrochim. Acta*, **22**, 1949 (1966).
- D. Potts, H. D. Sharma, A. J. Carty, and A. Walker, *Inorg. Chem.*, **13**, 1205 (1974).
- G. M. Bancroft, "Mössbauer Spectroscopy", McGraw-Hill, London, 1973, p 142.
- L. E. Levchuk, J. R. Sams, and F. Aubke, *Inorg. Chem.*, **11**, 43 (1972).

- (27) P. A. Yeats, B. F. E. Ford, J. R. Sams, and F. Aubke, *Chem. Commun.*, 791 (1969).
 (28) B. F. E. Ford, J. R. Sams, R. G. Goel, and D. R. Ridley, *J. Inorg. Nucl. Chem.*, 33, 23 (1971).
 (29) T. H. Tan, J. R. Dalziel, P. A. Yeats, J. R. Sams, R. C. Thompson, and F. Aubke, *Can. J. Chem.*, 50, 1843 (1972).
 (30) B. Gassenheimer and R. H. Herber, *Inorg. Chem.*, 8, 1120 (1969).
 (31) P. J. Smith, *Organomet. Chem. Rev.*, 5, 373 (1970).

Contribution from the Department of Chemistry,
 The Pennsylvania State University, University Park, Pennsylvania 16802

Ring-Ring and Ring-Chain Equilibration of Dimethylphosphazenes. Relationship to Phosphazene Polymerization^{1,2}

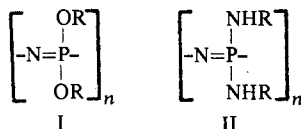
H. R. ALLCOCK* and D. B. PATTERSON

Received September 20, 1976

AIC60699R

Hexamethylcyclotriphosphazene, $[\text{NP}(\text{CH}_3)_2]_3$, and octamethylcyclotetraphosphazene, $[\text{NP}(\text{CH}_3)_2]_4$, participate in a ring-ring equilibration between 200 and 350 °C, but they do not polymerize. A ΔH value of 10.2 kcal and a ΔS value of 14.3 eu were determined for the tetramer-trimer interconversion. The equilibration is inhibited by base. Acids accelerate equilibration and also yield linear low molecular weight compounds: these species cyclize to III and IV when heated. The results are compared with the ring-high polymer and ring-ring interconversions in the halogenophosphazene, dimethylsiloxane, dimethylsilthiane, and polysulfur series.

The synthesis of high molecular weight poly(organo-phosphazenes) (I) and (II) by the nucleophilic replacement



of halogen in poly(dichlorophosphazene) has been described in earlier papers.³⁻¹¹ This earlier work¹¹ suggested that a marked increase in thermal stability might be anticipated if the substituent groups could be restricted to alkyl or aryl residues bonded directly to phosphorus. This viewpoint was based on the observation that bulky substituent groups (such as phenoxy) destabilized the polymer thermodynamically and favored depolymerization at high temperatures to cyclic oligomers. Moreover, the mechanisms of depolymerization and decomposition were believed to be connected with the presence of ionizable or displaceable groups such as alkoxy or aryloxy. Thus, a prime objective in phosphazene chemistry is the synthesis of high polymers that contain short alkyl or aryl residues as side units.

In an earlier paper we reported the synthesis of polymers that contained both phenyl and halogeno, alkoxy, or amino substituents.¹² However, up to the present no authentic linear high polymers have been reported which contain *only* alkyl or aryl substituent groups. The most definitive attempt was by Sisler, Frazier, Rice, and Sanchez,¹³ who reported the formation of oligomers or low polymers of dimethylphosphazene by the pyrolysis of dimethyldiaminophosphonium chloride.

Our interest in methylphosphazenes was prompted by the realization that the small steric size of the methyl group and the high bond strength of P—C bonds ($\text{Me}_3\text{P}=\text{O}$ can be heated without decomposition to 700 °C¹⁴) offered the prospect that the cyclic phosphazenes, $[\text{NP}(\text{CH}_3)_2]_3$ and 4 (III

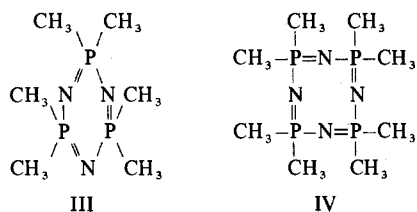


Table I. Equilibration of $[\text{NP}(\text{CH}_3)_2]_3$ and $[\text{NP}(\text{CH}_3)_2]_4$ ^a

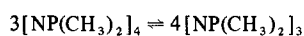
Temp, °C	Starting material	Re-action time, days	Final compn, mol %	
			$[\text{NP}(\text{CH}_3)_2]_3$	$[\text{NP}(\text{CH}_3)_2]_4$
346.5	$[\text{NP}(\text{CH}_3)_2]_3$	4	48.6	51.4
346.5	$[\text{NP}(\text{CH}_3)_2]_4$	4	45.4	54.6
250.0	$[\text{NP}(\text{CH}_3)_2]_3$ ^b	11	36.3	63.7
250.0	$[\text{NP}(\text{CH}_3)_2]_4$ ^b	11	37.1	62.9

^a In the molten bulk phase. ^b 1 wt % $[\text{NP}(\text{CH}_3)_2]_4 \cdot 2\text{HCl}$ added. Other reactions carried out in the absence of this reagent gave essentially the same result.

and IV), might be polymerizable to thermally stable linear high polymers. Earlier work had suggested that the polymerizability of $(\text{NPF}_2)_3$, $(\text{NPCl}_2)_3$, and $(\text{NPBr}_2)_3$ was connected with the presence of small, ionizable (or hydrolyzable) halogen substituents, while the nonpolymerizability of $[\text{NP}(\text{OC}_6\text{H}_5)_2]_3$ and $[\text{NP}(\text{C}_6\text{H}_5)_2]_4$ was connected with the relatively large steric size of the substituent groups.¹² On the other hand, it was thought possible that, although thermal ionization or hydrolysis of methyl groups from phosphorus was unlikely, the steric inhibition to polymerization would be far less than that found for alkoxy, aryloxy, or aryl groups.

Results and Discussion

Ring-Ring Equilibration. When pure $[\text{NP}(\text{CH}_3)_2]_3$ or $[\text{NP}(\text{CH}_3)_2]_4$ was heated, equilibration occurred to yield mixtures of the two. In no case was more than a trace (<1%) of higher cyclic oligomers formed during this process. As the temperature was raised from 200 to 349.5 °C (Table I), the proportion of trimer in the equilibrate increased markedly. For the equilibration system



it was calculated that $\Delta H = +10.2$ kcal and $\Delta S = +14.3$ eu. Thus, the trimer is destabilized by about 1 kcal/monomer unit.

This large value of ΔH could be explained in three ways. First, it is possible that the cyclic tetramer is in some way electronically stabilized to a greater degree than is the trimer. This explanation is difficult to accept because (a) the tetramer is known to be puckered (at least in the solid state)¹⁵ and (b) little or no evidence has been produced to suggest that the tetramer is electronically stabilized more than the trimer when